

Contents lists available at [ScienceDirect](http://ScienceDirect.com)

Journal of Cranio-Maxillo-Facial Surgery

journal homepage: www.jcmfs.com

Quantifying the effect of corrective surgery for trigonocephaly: A non-invasive, non-ionizing method using three-dimensional handheld scanning and statistical shape modelling

Naiara Rodriguez-Florez ^{a,b,*}, Özge K. Göktekin ^{a,b,1}, Jan L. Bruse ^{b,c}, Alessandro Borghi ^{a,b}, Freida Angullia ^{a,b}, Paul G.M. Knoop ^{a,b}, Maik Tenhagen ^{a,b}, Justine L. O'Hara ^b, Maarten J. Koudstaal ^{b,d}, Silvia Schievano ^{a,b,c}, N.U. Owase Jeelani ^{a,b}, Greg James ^{a,b}, David J. Dunaway ^{a,b}

^a UCL Great Ormond Street Institute of Child Health (Head: Prof. R. Smyth), London WC1N 1EH, United Kingdom

^b Craniofacial Unit, Great Ormond Street Hospital for Children NHS Trust, London WC1N 3JH, United Kingdom

^c UCL Institute of Cardiovascular Science (Head: Prof. A. Hingorani), Centre for Cardiovascular Imaging, London WC1E 6BT, United Kingdom

^d Department of Maxillofacial Surgery, Erasmus MC, 3015 CE Rotterdam, The Netherlands

ARTICLE INFO

Article history:

Paper received 27 July 2016

Accepted 3 January 2017

Available online xxx

Keywords:

Fronto-orbital remodelling

Trigonocephaly

3D scanning/photography

Statistical shape analysis

Principal component analysis

Craniosynostosis

ABSTRACT

Trigonocephaly in patients with metopic synostosis is corrected by fronto-orbital remodelling (FOR). The aim of this study was to quantitatively assess aesthetic outcomes of FOR by capturing 3D forehead scans of metopic patients pre- and post-operatively and comparing them with controls. Ten single-suture metopic patients undergoing FOR and 15 age-matched non-craniosynostotic controls were recruited at Great Ormond Street Hospital for Children (UK). Scans were acquired with a three-dimensional (3D) handheld camera and post-processed combining 3D imaging software. 3D scans were first used for cephalometric measurements. Statistical shape modelling was then used to compute the 3D mean head shapes of the three groups (FOR pre-op, post-op and controls). Head shape variations were described via principal component analysis (PCA). Cephalometric measurements showed that FOR significantly increased the forehead volume and improved trigonocephaly. This improvement was supported visually by pre- and post-operative computed mean 3D shapes and numerically by PCA ($p < 0.001$). Compared with controls, post-operative scans showed flatter foreheads ($p < 0.001$). In conclusion, 3D scanning followed by 3D statistical shape modelling enabled the 3D comparison of forehead shapes of metopic patients and non-craniosynostotic controls, and demonstrated that the adopted FOR technique was successful in correcting bitemporal narrowing but overcorrected the rounding of the forehead.

© 2017 The Author(s). Published by Elsevier Ltd on behalf of European Association for Cranio-Maxillo-Facial Surgery. This is an open access article under the CC BY license (<http://creativecommons.org/licenses/by/4.0/>).

1. Introduction

Craniosynostosis is a condition in which one or more cranial sutures fuse prematurely, leading to an abnormal head shape. Premature fusion of the metopic suture leads to bitemporal narrowing with a compensatory increase in cephalic width, resulting in trigonocephaly. Other characteristics include midline ridging, hypotelorism, teardrop-shaped orbits, and depressed orbital rims

(Beckett et al., 2012; Birgfeld et al., 2013). The surgical procedure used to correct trigonocephaly in single-suture metopic synostosis at Great Ormond Street Hospital for Children (GOSH, London, UK) is fronto-orbital remodelling (FOR) (James et al., 2015).

The assessment of the aesthetic outcome of FOR is often subjective, depending on the clinicians' and/or parents' visual judgment and satisfaction (Anand et al., 2013; Britto et al., 2012; Metzler et al., 2013; Szpalski et al., 2011; Ul Haq et al., 2014). In order to quantify head shape changes achieved by FOR, pre- and post-operative 3D images of the forehead are required. Traditional methods include computed tomography (CT) scans followed by cephalometric measurements (Ezaldein et al., 2014; Metzler et al., 2014; Oi and Matsumoto, 1987; Posnick et al., 1994). Due to concerns about the deleterious effects of exposure to ionizing radiation

* Corresponding author. SCRM Section, Room 160 Developmental Biology and Cancer Programme, UCL GOS Institute of Child Health, 30 Guilford Street, London WC1N 1EH, United Kingdom.

E-mail address: n.florez@ucl.ac.uk (N. Rodriguez-Florez).

¹ N.R.F and Ö.K.G contributed equally to this work.

<http://dx.doi.org/10.1016/j.jcms.2017.01.002>

1010-5182/© 2017 The Author(s). Published by Elsevier Ltd on behalf of European Association for Cranio-Maxillo-Facial Surgery. This is an open access article under the CC BY license (<http://creativecommons.org/licenses/by/4.0/>).

Please cite this article in press as: Rodriguez-Florez N, et al., Quantifying the effect of corrective surgery for trigonocephaly: A non-invasive, non-ionizing method using three-dimensional handheld scanning and statistical shape modelling, Journal of Cranio-Maxillo-Facial Surgery (2017), <http://dx.doi.org/10.1016/j.jcms.2017.01.002>

in infants, in addition to the routine use of general anaesthesia for many of these scans, our group has not used routine CT scanning (either pre- or post-operatively) for uncomplicated single-suture synostosis cases for more than a decade (Cerovac et al., 2002). Other groups have also reported that the routine use of CT in metopic synostosis is non-contributory (Engel et al., 2012).

Three-dimensional (3D) scanning has become an attractive technique to assess head shape changes following craniofacial surgery in a non-invasive, ionizing radiation-free and anaesthetic-free manner (Kau et al., 2007; Linz et al., 2014; Martini et al., 2015; McKay et al., 2010; Schaaf et al., 2010; Wong et al., 2008). Few studies have used 3D photogrammetry to capture pre- and post-operative scans of metopic patients undergoing FOR in order to perform cephalometric measurements (i.e. volume, frontal angle, head circumference) (Freudlsperger et al., 2015; Martini et al., 2015; Wilbrand et al., 2012). Although these measurements provide valuable information about the effects of surgery, they do not describe regional and global surface shape features of the forehead in a 3D fashion.

The aim of our study was to capture pre- and post-operative head shapes of metopic patients undergoing FOR at GOSH using a 3D handheld scanner to quantitatively assess 3D head shape changes induced by surgery. Our approach allowed visual and quantitative shape assessment by computing mean pre- and post-operative head shapes and describing their 3D shape variability using a non-parametric statistical shape modelling (SSM) technique (Durrleman et al., 2014). Since the 3D handheld scanner is a safe and portable tool, its use was extended to acquire scans of age-matched, non-craniosynostotic controls to compare their head shape with the post-operative shapes of the metopic cohort. We hypothesized that quantifying the 3D head shape of patients before and after FOR and comparing those shapes to those of controls could provide valuable insight for future surgical planning and assessment of surgical outcome.

2. Material and methods

2.1. Patients and surgical technique

Ten consecutive metopic patients (9 male, 1 female; mean age 17.3 ± 3.1 months) who underwent FOR, and 15 non-craniosynostotic controls (11 male, 4 female; mean age 21.1 ± 3.2 months) who underwent non-craniofacial (e.g. gastro-intestinal, urologic) operations at GOSH were recruited prospectively between October 2015 and March 2016. Informed consent was given for the 3D scans to be acquired and used for scientific publication. Local and ethical procedures were followed.

Our standard technique for FOR correction for trigonocephaly is the “Hayward technique” (James et al., 2015). In brief, a bicoronal retroauricular scalp incision is made, and the scalp is elevated to the orbital rims bilaterally in one or two layers. A favourable contour for the new supra-orbital region is selected from the posterior region of the fronto-parietal bones, which is then used to plan the bifrontal craniotomy. Following elevation of the bifrontal bone flap, the deformed supra-orbital rims and temporal squames are resected. The bifrontal bone flap is then divided into 2 halves and rotated 180° , and the sides are swapped to form a new supraorbital contour. Once optimal positioning is achieved, the flaps are secured with a combination of dental wire (basally) and resorbable sutures (vertex). Further tailoring of the final result is achieved with further “armadillo”-style osteotomies as required. Any bony defects are filled with a morcellized bone paste (formed using fibrin glue, “bone salami”) (Rashid et al., 2008). The wound is closed in layers with resorbable sutures.

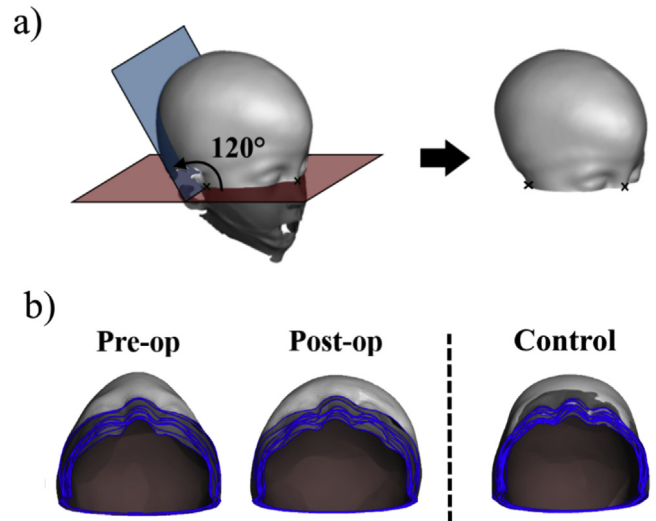


Fig. 1. a) Scans were cut by a base plane through the cruses of helix and the nasion (in red) and a second plane 120° posterior to the base plane (in blue) through the cruses of helix. b) Cut pre-operative, post-operative and control scans were registered according to the cruses of helix along the base plane.

2.2. 3D scans: image acquisition and processing

3D scans of metopic patients were acquired pre- and post-operatively in theatre using a structured light handheld scanner (M4D Scanner, Rodin4D, Pessac, France) connected to a laptop with VXelements software (Creaform, Levis, Quebec, Canada). Scans of non-craniosynostotic controls were performed in the anaesthetic room after administration of general anaesthesia or in the ward while patients were waiting to be called for surgery. The scanner was calibrated regularly to ensure that differences in the rooms in which the images were acquired did not influence the results. Since structured light handheld cameras have difficulties capturing hair, tight white nylon stockings (Beagle Orthopaedic, UK) were used to cover patient hair.

The scans were exported as 3D computational surface meshes in stereolithography (STL) format for post-processing (Fig. 1). All post-processing was done by the same examiner. Artefacts and objects outside the region of interest were cleaned up using MeshMixer software (Autodesk Inc., Toronto, ON, Canada). In cases in which the camera did not capture the full head in one scan, multiple scans were merged together using 3-matic (Materialise, Leuven, Belgium).

Images were cut by planes defined by facial anatomical landmarks (Robin's 3D Image Rendering Software package, UK) in order to capture the surgically remodelled area (Fig. 1a). A base plane was created through the left and right crus of helix and the nasion, as these landmarks are not expected to change during the surgical intervention. It must be noted that although in some FOR procedures the nasion might be affected by the surgery (Britto et al., 2012), osteotomies in the so-called Hayward technique are performed in the supra-orbital region (James et al., 2015) and, hence, the nasion remains unchanged. To capture the full forehead, a second plane was created 120° from the first plane towards the posterior through the cruses of helix. The reliability of the three landmarks used to define the planes was assessed by locating them 10 times on the same scan leaving at least 12 h between measurements. The intra-class correlation (ICC) was $ICC > 0.99$ ($p < 0.001$), indicating an excellent intra-rater reliability of the chosen landmarks.

In order to directly compare head shapes in 3D, the acquired scans were registered (rigidly aligned on top of each other), using the crus of helixes along the base plane (3-matic, Fig. 1b). First, all

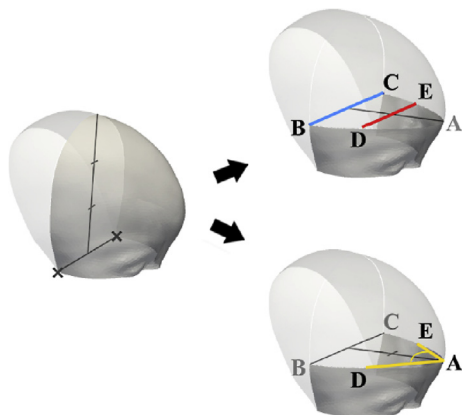


Fig. 2. Measurements are taken on a plane parallel to the base plane at one-third of the forehead height. The interfrontoparietal–interparietal ratio (top) is defined by $\overline{DE}/\overline{BC}$ while the frontal angle (bottom) is defined by \overline{DAE} .

pre-operative scans were registered; each post-operative scan was then registered to the corresponding pre-operative scan; and finally, control scans were registered to the average post-operative scan.

2.3. Cephalometric measurements

The following cephalometric parameters were measured on the 3D scans (Rhinoceros 3D software, Robert McNeel & Associates, Seattle, WA, USA): forehead volume defined by the volume between the base plane and the posterior plane at 120° (Fig. 1a); interfrontoparietal–interparietal ratio and frontal angle (Fig. 2) to assess the narrowing of the fronto-temporal region and rounding of the forehead, which are the regions of correction in metopic patients. The ratio and the angle were measured on a plane parallel to the base plane at one-third of the head height. This plane was chosen as it included the most anterior point of the forehead in metopic patients (glabella), which was referred to as point A. The interparietal distance (\overline{BC}) (Fig. 2) was defined as the width of the forehead parallel to the line that connects the left and right crus of helix. The interfrontoparietal distance (\overline{DE}) (Fig. 2) was defined as the width of the skull half distance from \overline{BC} to A. Therefore, as shown in Fig. 2, the interfrontoparietal–interparietal ratio was computed as $\overline{DE}/\overline{BC}$, whereas the frontal angle was measured as \overline{DAE} .

2.4. Statistical shape modelling: average models and principal component analysis

A non-parametric statistical shape modelling (SSM) approach that does not require manual landmarking was used to compute the 3D anatomical mean head shapes of pre- and post-operative FOR patients as well as of controls (Deformetrica, www.deformetrica.org) (Bruse et al., 2016; Durrleman et al., 2014). The method simultaneously computes the mean shape of a 3D shape population and the deformation vectors, deforming the mean shape towards each of the included subject shapes. Mean and deformation vectors thus numerically describe all 3D head shape features of the population and allow statistical analyses of 3D shapes within a coherent framework.

The registered 3D scans (Fig. 1b) were used to compute separate mean shapes for each of the shape populations (pre-operative, post-operative and controls) to obtain average head shape features characteristic for each of the groups. To check the robustness of the technique and to ensure that the final average shapes were not

overly influenced by adding or leaving out one specific shape, k-fold cross-validation was performed for each of the average models (Bruse et al., 2016; Mansi et al., 2011). This involved leaving one patient out of the analysis each time and re-computing the average model, until each patient had been excluded once. Surface distances between mean pre-, post- and control scans were calculated using VMTK (The Vascular Modeling Toolkit, Bergamo, Italy) (Antiga et al., 2008) and visualized in ParaView (Ahrens et al., 2005) (Kitware, Clifton Park, NY, USA).

Traditionally, 3D shape variability around the computed mean shape is described via principal component analysis (PCA) (Heimann and Meinzer, 2009; Jolliffe, 2002), which can be applied to analyse craniofacial abnormalities (Crombag et al., 2014; Staal et al., 2015). This mathematical technique allows one to break down high-dimensional shape variability into a smaller subset of so-called shape modes that characterize the dominant contributors to 3D shape variability within the dataset. Each shape mode accounts for a certain percentage of total shape variability and can be visualized as a deformation of the mean shape. Furthermore, the so-called shape vector (Mansi et al., 2011) numerically quantifies how much of the shape features described by a specific shape mode is contained within a subject head shape. Low shape vector values thereby relate to a small deformation of the mean shape along the mode, while high shape vector values relate to large deformations. In summary, shape modes allow visualization of principal 3D shape features present in the population, and shape vectors allow quantification of those 3D shape features with respect to an individual's head shape, thus allowing statistical analysis of shape.

To quantitatively compare all three groups, a joint statistical shape model was computed in Deformetrica, using all 35 head scans as input. PCA was carried out on the derived deformation vectors (Matlab, Mathworks, Natick, MA, USA), and shape modes were visualized as deformation of the obtained mean shape from -2 standard deviations (-2σ) to $+2\sigma$ for the respective shape mode. Shape vector values were computed for each mode and compared among the three groups via traditional statistical analysis.

2.5. Statistical analysis

Mean values and standard deviations were calculated for the measured parameters (forehead volume, interfrontoparietal–interparietal ratio, frontal angle) and PCA shape vectors. The Wilcoxon signed-rank paired test was used to compare pre- and post-operative measurements of metopic patients. Measurements on controls were compared to pre- and post-operative measurements of FOR patients via an independent Mann–Whitney U test. Differences were considered significant at $p < 0.05$. Statistical analysis was performed using SPSS (v.22, SPSS Inc. Chicago, IL, USA).

3. Results

3D head scans of metopic patients immediately before and after FOR as well as non-craniosynostotic controls were acquired successfully with the handheld scanner. Fig. 3 shows overlaid top-down views of individual pre- and post-operative forehead scans of metopic patients, demonstrating overall shape change following surgical correction.

3.1. Cephalometric measurements

Mean and standard deviations of the cephalometric measurements of forehead volume, interfrontoparietal–interparietal ratio and frontal angle are summarised in Fig. 4. Forehead volume increased from pre-operative ($1265 \pm 168 \text{ cm}^3$) to post-operative

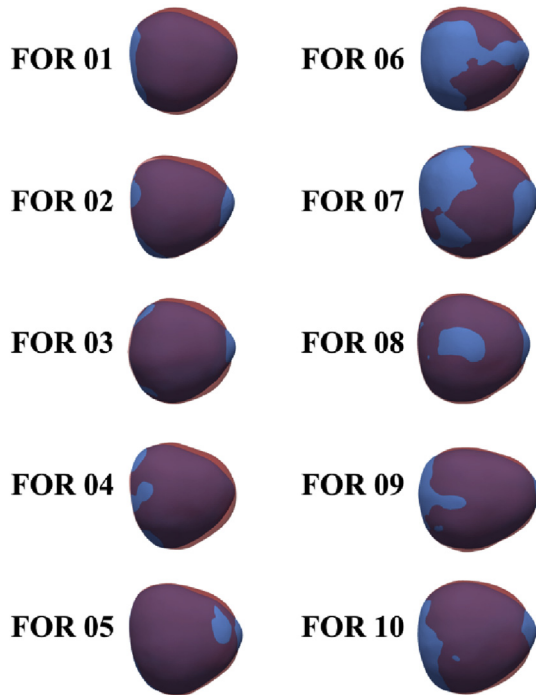


Fig. 3. Top view of the forehead scans of the ten metopic patients pre- (in blue) and post- (in red) fronto-orbital remodelling (FOR).

($1378 \pm 165 \text{ cm}^3$) scans for all patients ($p = 0.007$). No statistically significant differences were found between pre-operative and control volumes or between post-operative and control volumes (mean control volume: $1243 \pm 146 \text{ cm}^3$). The interfrontoparietal–interparietal ratio ($\overline{DE/BC}$) increased from pre-operative to post-operative scans ($p = 0.005$) and was significantly different between the pre-operative and control groups ($p < 0.001$), but not between the post-operative and control groups. The frontal angle (\overline{DAE}) widened significantly from pre-operative to post-operative scans ($p = 0.005$). Compared to the frontal angle of control scans, pre-operative scans had a narrower angle ($p < 0.001$), whereas post-operative scans had a wider angle than controls ($p = 0.002$).

3.2. Average models

The chosen non-landmark-based SSM approach computed the mean shapes of pre-operative, post-operative and control scans, demonstrating the effects of FOR surgery on forehead shape (Fig. 5).

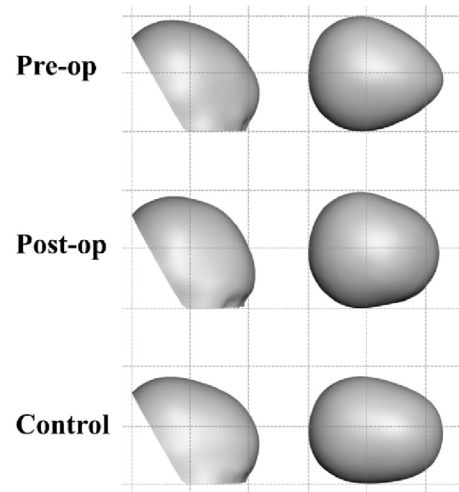


Fig. 5. Lateral and top views of the computed mean shape models of fronto-orbital remodelling (FOR) patients pre- and post-operatively and non-craniosynostotic controls.

The leave-one-out cross-validations showed that none of the average models was overly influenced by any individual scan.

The regional differences in the three mean shape models are quantified by surface distance maps in Fig. 6. The colour maps indicate that, on average, metopic patients pre-operatively had 10 mm wider parietal width and a bitemporal narrowing of 10 mm on each side when compared to those of controls (Fig. 6, top). During FOR, the metopic ridge was decreased on average by 5 mm, and the sides of the forehead were augmented by 10 mm (Fig. 6, middle). Comparing the mean post-operative head shape to the mean control shape, the central portion of the forehead was 10 mm flatter and the parietal width was 10 mm wider (Fig. 6, bottom).

3.3. Principal component analysis

After performing PCA including all pre-operative, post-operative and control scans, the first three modes of variations represented 68% of the total shape variability within the population. The top part of Fig. 7 shows the deformation of two standard deviations down (-2σ) and two standard deviations up ($+2\sigma$) from the computed mean shape for the first three shape modes. Shape deformations towards -2σ relate to low values of the corresponding PCA shape vector, whereas deformations towards $+2\sigma$ relate to high shape vector values.

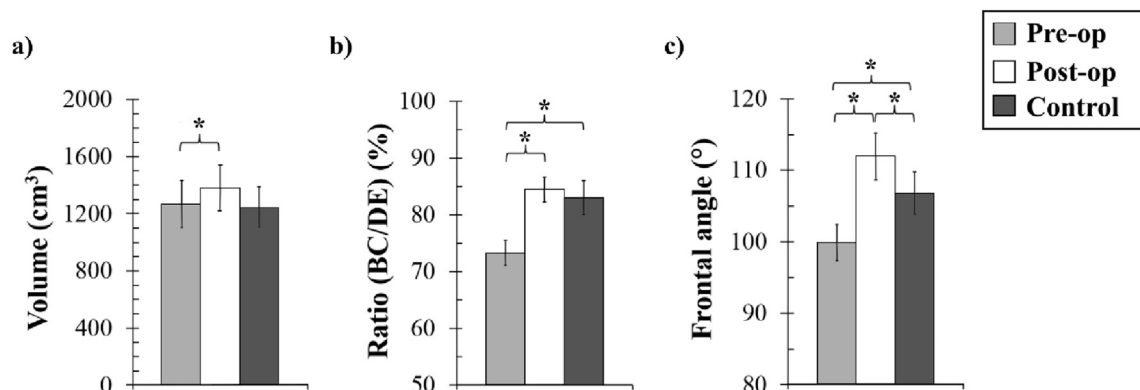


Fig. 4. Average and standard deviations of a) forehead volume, b) interfrontoparietal–interparietal ratio, and c) frontal angle, measured on the 3D scans. * $p < 0.05$.

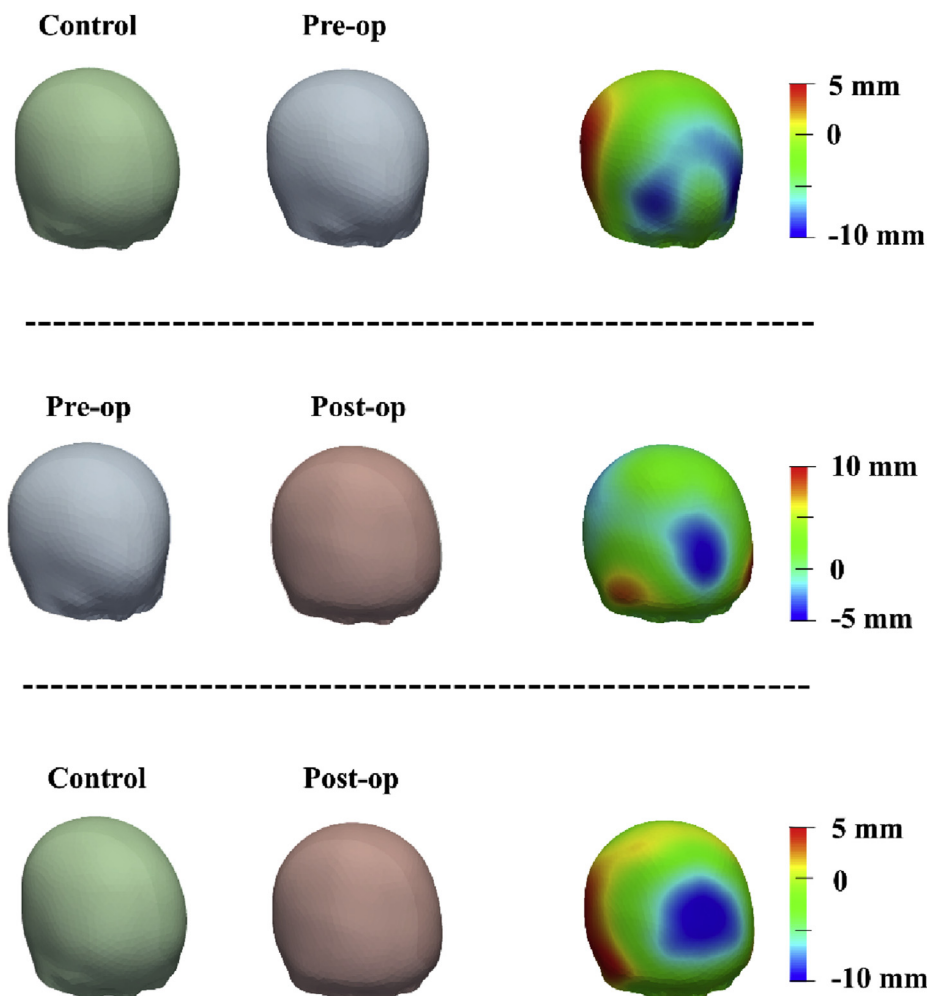


Fig. 6. Surface distance maps between pre-operative and control (top), post- and pre-operative (middle), and post-operative and control (bottom) average models. Positive numbers represent an augmentation from the left scan to the right scan.

The first shape mode (Mode 1) captured overall head size combined with the roundness of the forehead, as shown in Fig. 7a. Pre-operative scans were associated with lower values of Mode 1, indicating smaller and more elliptical foreheads, whereas post-operative scans were linked to higher values matching larger and rounder foreheads ($p = 0.005$). No significant differences were found between shape vector values associated with pre-operative scans and controls or between post-operative values and controls.

The second shape mode (Fig. 7b) captured the differences in the interparietal width and flatness of the frontal part of the forehead. This highlighted mainly the difference between control scans, closest to the -2σ model, and post-operative scans, related to the $+2\sigma$ model ($p < 0.001$). Pre-operative scans were in between, with wider interparietal width than those of controls ($p = 0.046$), but a rounder frontal part of the forehead than on post-operative scans ($p = 0.005$).

The effects of FOR, the widening of the interfrontoparietal width and the frontal angle were best represented in the third shape mode (Fig. 7c). There was a significant difference between pre-operative scans and those of controls ($p = 0.005$) due to the triangular forehead shape of metopic patients. This was improved from pre-operative to post-operative scans ($p < 0.001$), but the shape mode revealed an over-effacing of the forehead when post-operative scans were compared to those of controls ($p = 0.02$).

4. Discussion

In this study, pre-operative and post-operative scans of metopic patients undergoing FOR as well as age-matched non-craniosynostotic controls were successfully acquired using a structured light 3D handheld scanner. Both the cephalometric measurements and, for the first time, the computation of 3D anatomical mean forehead shapes of metopic patients and age-matched controls allowed numerical and statistical analysis. Comparison of the three groups revealed that the adopted FOR technique is successful in correcting bitemporal narrowing but overcorrects the rounding of the forehead.

The main novelty of this study lies in the use of a SSM technique to characterise the “average” effects of surgery in our cohort by comparing mean 3D forehead shapes of pre-operative, post-operative and control scans (Figs. 5 and 6) and performing PCA to describe and quantify 3D head shape variability (Fig. 7). This provides the advantage of visualising and statistically analysing 3D shape differences in the three groups from a population perspective. Furthermore, rigorous registration protocol allowed the calculation of surface distance maps that intuitively quantify and visualise 3D shape changes induced by surgery as well as shape differences between metopic and non-craniosynostotic forehead shapes (Fig. 6).

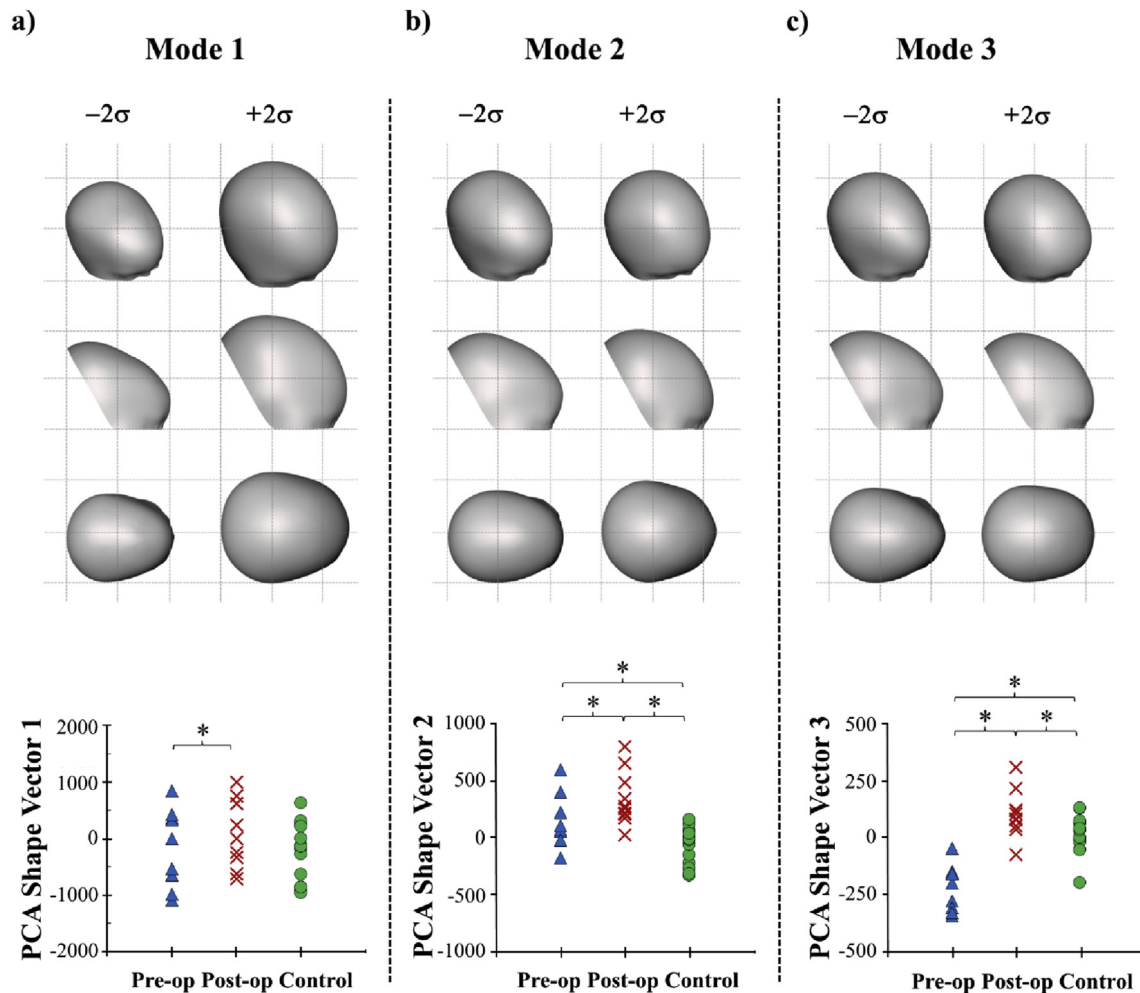


Fig. 7. Visual (top) and numerical (bottom) results of the first three modes of variation after applying principal component analysis (PCA) to pre-operative, post-operative and control scans. Each mode of variation is represented by shape models that vary -2σ to $+2\sigma$ from the average model. Low values of PCA shape vectors are associated with shape models closer to -2σ , while high shape vector values are related to shapes closer to $+2\sigma$. * $p < 0.05$.

Results showed that, pre-operatively, metopic patients had a lower interfrontoparietal–interparietal ratio and narrower frontal angle than controls (Fig. 4), which was visualised, in 3D, in the distance maps between the computed mean control and pre-operative shapes (Fig. 6, top). Statistically, pre-operative scans were associated with significantly wider interparietal width (described by the second PCA shape mode, Mode 2) and more triangular forehead shape (Mode 3) than controls. These results are in accordance with descriptions of trigonocephaly found in the literature (Anderson et al., 1962; Birgfeld et al., 2013; Ezaldeen et al., 2014; Posnick et al., 1994; van der Meulen, 2012).

Cephalometric measurements on metopic patients before and after FOR suggested that surgery improved trigonocephaly, as the interfrontoparietal–interparietal ratio increased and the frontal angle widened (Fig. 4). Similar results have also been reported in measurements on CT scans (Beckett et al., 2012; Ezaldeen et al., 2014; Kellogg et al., 2012; Metzler et al., 2014) and 3D photos (Freudspurger et al., 2015; Martini et al., 2015; Wilbrand et al., 2012) of metopic patients undergoing different FOR interventions. Information from cephalometric measurements was complemented, for the first time, by 3D visualisation of the mean differences in the forehead shape of metopic patients before and after FOR (Fig. 6, middle). Surface distance maps showed that there is a temporal widening and a decrease in the metopic ridge from mean

pre-operative to post-operative scans. The third shape mode demonstrated that FOR significantly improves the frontal triangular forehead shape of metopic patients. The increase in forehead size, captured in the first shape mode, was in accordance with the increase in forehead volume measured from pre-operative to post-operative scans. Although FOR is performed for aesthetic purposes, it is interesting to note that in this study the volume increased from pre-operative to post-operative scans in all metopic patients. While clinically significant raised intracranial pressure is rare in single-suture metopic synostosis (Thompson et al., 1995), it seems intuitive that increasing rather than decreasing intracranial volume is desirable when operating on these children.

Although FOR improved the overall trigonocephalic shape, post-operative scans had significantly wider frontal angle than controls (Fig. 4) due to the fact that the frontal part of the forehead was overcorrected (Figs. 5 and 6, bottom). This was best described by the second shape mode, which ranged from more rounded foreheads (associated with controls) to wider shapes with flatter forehead (associated with post-operative scans). The inherent shape of the bone flaps predicts resultant forehead shape with the advantage of bone curvature used to fill lateral emptiness and match to widened temporal regions. It is the usual practice in our unit to “overcorrect” the temporal narrowness during FOR, to prevent the well-described “temporal hollowing” that can be a late finding in these children (van

der Meulen et al., 2009; Wes et al., 2014). This leads to an exaggerated augmentation of the lateral supraorbital region and may explain some of the increased flatness of forehead seen in the current series. One of the advantages of the technique described in this report is that it will allow long-term, non-ionizing, 3D follow-up of this patient cohort to further examine the results of our FOR technique and allow further refinement.

The future use of 3D handheld cameras to capture scans that will then be analysed by SSM could be extended to a broader audience if the post-processing were faster. In this study, the post-processing involved combining several 3D imaging software to clean, cut and register the scans (Fig. 1). This workflow could be improved by integrating the different steps within one software program and even automating part of the process.

The main limitation of our study is the relatively small sample size of both the control and metopic patient groups, which should be addressed by future studies. However, thanks to the safety and portability of 3D handheld scanners, we predict a build-up of 3D head scan databases in clinical centres, allowing more refined, population-based analysis of cranio-maxillofacial outcome on a larger scale.

This study showcased the potential of 3D scanning followed by 3D shape modelling, especially advantageous when including controls in the study. Having a handheld camera that could capture 3D images in a safe and non-invasive manner facilitated the recruitment of age-matched non-craniosynostotic controls. Furthermore, previous head shape comparisons between metopic patients and controls have been limited to comparisons between cephalometric measurements (Anderson et al., 2004; Ezaldein et al., 2014; Gociman et al., 2014; Kellogg et al., 2012; Wang et al., 2016) or visual one-to-one comparisons of a metopic patient with one age-matched control (Britto et al., 2012). The proposed method computed a joint statistical model including forehead shapes of 10 metopic patients and 15 controls in order to visualise and quantify 3D shape differences in the population.

5. Conclusion

To the best of our knowledge, this is the first study to quantify and to demonstrate in a 3D fashion that FOR improves trigonocephaly in metopic patients, bringing the head shape of those patients closer to the shape of non-craniosynostotic controls. However, it also highlighted the areas requiring improvement, as it revealed that the frontal part of the forehead is overcorrected in FOR, leading to post-operative foreheads that are flatter than those of controls. This study provides a quantification of the average differences between controls and metopic patients just before and after undergoing FOR and provides detailed insight into 3D head shape features differentiating those three groups, which is essential to evaluate and improve current surgical techniques.

The methods presented in this study could also be implemented in other craniofacial and reconstructive interventions, as non-invasive and radiation-free 3D scanning followed by statistical 3D shape analysis provides a powerful tool to visualise and to quantify global and regional surface shape changes achieved in craniofacial surgery.

Conflict of interest

The authors declare that they have no conflict of interest in regard to this work.

Acknowledgements

This research was supported by Great Ormond Street Hospital charity through the FaceValue programme grant (no. 508857), the

Engineering and Physical Sciences Research Council award (EP/N02124X/1), and Fondation Leducq. This report incorporates independent research from the National Institute for Health Research Biomedical Research Centre Funding Scheme. The views expressed in this publication are those of the author(s) and not necessarily those of the NHS, the National Institute for Health Research or the Department of Health.

References

- Ahrens J, Geveci B, Law C: ParaView: an end-user tool for large data visualization. *Energy* 836: 717–732, 2005
- Anand A, Campion NJ, Cheshire J, Haigh T, Leckenby J, Nishikawa H, et al: Analysis of cosmetic results of metopic synostosis: concordance and interobserver variability. *J Craniofac Surg* 24: 304–308. <http://dx.doi.org/10.1097/SCS.0b013e318272d2ad>, 2013
- Anderson FM, Gwinn JL, Todt JC: Trigenocephaly. Identity and surgical treatment. *J Neurosurg* 19: 723–730. <http://dx.doi.org/10.3171/jns.1962.19.9.0723>, 1962
- Anderson PJ, Netherway DJ, Abbott A, David DJ: Intracranial volume measurement of metopic craniosynostosis. *J Craniofac Surg* 15: 1014–1016, 2004 1018
- Antiga L, Piccinelli M, Botti L, Ene-Iordache B, Remuzzi A, Steinman DA: An image-based modeling framework for patient-specific computational hemodynamics. *Med Biol Eng Comput* 46: 1097–1112. <http://dx.doi.org/10.1007/s11517-008-0420-1>, 2008
- Beckett JS, Chadha P, Persing JA, Steinbacher DM: Classification of trigonocephaly in metopic synostosis. *Plast Reconstr Surg* 130: 442e–447e. <http://dx.doi.org/10.1097/PRS.0b013e31825dc244>, 2012
- Birgfeld CB, Saltzman BS, Hing AV, Heike CL, Khanna PC, Gruss JS, et al: Making the diagnosis: metopic ridge versus metopic craniosynostosis. *J Craniofac Surg* 24: 178–185. <http://dx.doi.org/10.1097/SCS.0b013e31826683d1>, 2013
- Britto JA, Gwanmesia I, Leshem D: The Christmas tree foreheadplasty: a novel technique used in combination with a bandeau for fronto-orbital remodelling in craniosynostosis. *Childs Nerv Syst* 28: 1375–1380. <http://dx.doi.org/10.1007/s00381-012-1806-9>, 2012
- Bruse JL, McLeod K, Biglino G, Ntsinjana HN, Capelli C, Hsia T-Y, et al: A statistical shape modelling framework to extract 3D shape biomarkers from medical imaging data: assessing arch morphology of repaired coarctation of the aorta. *BMC Med Imaging* 16. <http://dx.doi.org/10.1186/s12880-016-0142-z>, 2016
- Cerovac S, Neil-Dwyer JG, Rich P, Jones BM, Hayward RD: Are routine preoperative CT scans necessary in the management of single suture craniosynostosis? *Br J Neurosurg* 16: 348–354, 2002
- Crombag GAJC, Verdoorn MHAS, Nikkha D, Ponniah AJT, Ruff C, Dunaway D: Assessing the corrective effects of facial bipartition distraction in Apert syndrome using geometric morphometrics. *J Plast Reconstr Aesthet Surg* 67: e151–e161. <http://dx.doi.org/10.1016/j.bjps.2014.02.019>, 2014
- Durrleman S, Prastawa M, Charon N, Korenberg JR, Joshi S, Gerig G, et al: Morphometry of anatomical shape complexes with dense deformations and sparse parameters. *NeuroImage* 101: 35–49. <http://dx.doi.org/10.1016/j.neuroimage.2014.06.043>, 2014
- Engel M, Castrillon-Oberndorfer G, Hoffmann J, Freudlsperger C: Value of preoperative imaging in the diagnostics of isolated metopic suture synostosis: a risk-benefit analysis. *J Plast Reconstr Aesthetic Surg JPRAS* 65: 1246–1251. <http://dx.doi.org/10.1016/j.bjps.2012.03.038>, 2012
- Ezaldein HH, Metzler P, Persing JA, Steinbacher DM: Three-dimensional orbital dysmorphology in metopic synostosis. *J Plast Reconstr Aesthet Surg* 67: 900–905. <http://dx.doi.org/10.1016/j.bjps.2014.03.009>, 2014
- Freudlsperger C, Steinmacher S, Bächli H, Somlo E, Hoffmann J, Engel M: Metopic synostosis: measuring intracranial volume change following fronto-orbital advancement using three-dimensional photogrammetry. *J Craniomaxillofac Surg* 43: 593–598. <http://dx.doi.org/10.1016/j.jcms.2015.02.017>, 2015
- Gociman B, Blagg R, Agko M, Goodwin I, Kestle JRW, Siddiqi F: The metopic angle: a novel assessment tool of the trigonocephalic frontal deformity and its correction. *J Craniofac Surg* 25: 2101–2104. <http://dx.doi.org/10.1097/SCS.0000000000001047>, 2014
- Heimann T, Meinzer H-P: Statistical shape models for 3D medical image segmentation: a review. *Med Image Anal* 13: 543–563. <http://dx.doi.org/10.1016/j.media.2009.05.004>, 2009
- James G, Jeelani NOU, Dunaway D, Hayward R: "A bandeau abandoned", an alternative fronto-orbital remodelling technique: report of 328 cases; 2015, Presented at the The 16th Congress of International Society of Craniofacial Surgery
- Jolliffe IT: *Principal component analysis*, Springer series in statistics. New York: Springer-Verlag, 2002
- Kau CH, Richmond S, Incrapera A, English J, Xia JJ: Three-dimensional surface acquisition systems for the study of facial morphology and their application to maxillofacial surgery. *Int J Med Robot* 3: 97–110. <http://dx.doi.org/10.1002/rcs.141>, 2007
- Kellogg R, Allori AC, Rogers GF, Marcus JR: Interfrontal angle for characterization of trigonocephaly: part 1. *J Craniofac Surg* 23: 799–804. <http://dx.doi.org/10.1097/SCS.0b013e3182518ad2>, 2012
- Linz C, Meyer-Marcotty P, Böhm H, Müller-Richter U, Jager B, Hartmann S, et al: 3D stereophotogrammetric analysis of operative effects after broad median

- craniectomy in premature sagittal craniosynostosis. *Childs Nerv Syst* 30: 313–318. <http://dx.doi.org/10.1007/s00381-013-2253-y>, 2014
- Mansi T, Voigt I, Leonardi B, Pennec X, Durrleman S, Sermesant M, et al: A statistical model for quantification and prediction of cardiac remodelling: application to tetralogy of Fallot. *IEEE Trans Med Imaging* 30: 1605–1616. <http://dx.doi.org/10.1109/TMI.2011.2135375>, 2011
- Martini M, Schulz M, Röhrig A, Nadal J, Messing-Jünger M: A 3D morphometric follow-up analysis after frontoorbital advancement in non-syndromic craniosynostosis. *J Craniomaxillofac Surg* 43: 1428–1437. <http://dx.doi.org/10.1016/j.jcms.2015.07.018>, 2015
- McKay DR, Davidge KM, Williams SK, Ellis LA, Chong DK, Teixeira RP, et al: Measuring cranial vault volume with three-dimensional photography: a method of measurement comparable to the gold standard. *J Craniofac Surg* 21: 1419–1422. <http://dx.doi.org/10.1097/SCS.0b013e3181e92a>, 2010
- Metzler P, Ezaldein HH, Persing JA, Steinbacher DM: Comparing two fronto-orbital advancement strategies to treat trigonocephaly in metopic synostosis. *J Craniomaxillofac Surg* 42: 1437–1441. <http://dx.doi.org/10.1016/j.jcms.2014.04.006>, 2014
- Metzler P, Zemmann W, Jacobsen C, Lübbers H-T, Grätz KW, Obwegeser JA: Assessing aesthetic outcomes after trigonocephaly correction. *Oral Maxillofac Surg* 18: 181–186. <http://dx.doi.org/10.1007/s10006-013-0399-0>, 2013
- Oi S, Matsumoto S: Trigocephaly (metopic synostosis). *Clinical, surgical and anatomical concepts. Childs Nerv Syst* 3: 259–265, 1987
- Posnick JC, Lin KY, Chen P, Armstrong D: Metopic synostosis: quantitative assessment of presenting deformity and surgical results based on CT scans. *Plast Reconstr Surg* 93: 16–24, 1994
- Rashid A, Marucci DD, Dunaway DJ, Hayward RD: Bone “salami”: morcellised bone and fibrin glue for filling extensive cranial defects in craniofacial surgery. *J Plast Reconstr Aesthet Surg* 61: 993–996. <http://dx.doi.org/10.1016/j.bjps.2007.10.056>, 2008
- Schaaf H, Pons-Kuehnemann J, Malik CY, Streckbein P, Preuss M, Howaldt H-P, et al: Accuracy of three-dimensional photogrammetric images in non-synostotic cranial deformities. *Neuropediatrics* 41: 24–29. <http://dx.doi.org/10.1055/s-0030-1255060>, 2010
- Staal FCR, Ponniah AJT, Angullia F, Ruff C, Koudstaal MJ, Dunaway D: Describing Crouzon and Pfeiffer syndrome based on principal component analysis. *J Craniomaxillofac Surg* 43: 528–536. <http://dx.doi.org/10.1016/j.jcms.2015.02.005>, 2015
- Szpalski C, Weichman K, Sagebin F, Warren SM: Need for standard outcome reporting systems in craniosynostosis. *Neurosurg Focus* 31: E1. <http://dx.doi.org/10.3171/2011.6.FOCUS1192>, 2011
- Thompson DN, Malcolm GP, Jones BM, Harkness WJ, Hayward RD: Intracranial pressure in single-suture craniosynostosis. *Pediatr Neurosurg* 22: 235–240, 1995
- Ul Haq E, Aslam A, Kazmi A, Tammimy MS, Aman S, Ahmad RS: Fronto-orbital advancement and total calvarial remodelling for craniosynostosis. *J Coll Physicians Surg Pak JCPSP*: 118–122. <http://dx.doi.org/10.2014/JCPSP.118122>, 2014
- van der Meulen J: Metopic synostosis. *Childs Nerv Syst* 28: 1359–1367. <http://dx.doi.org/10.1007/s00381-012-1803-z>, 2012
- van der Meulen JJNM, Willemsen J, van der Vlugt J, Nazir PRN, Hilling D, Mathijssen IMJ, et al, Dutch Craniofacial Unit: On the origin of bitemporal hollowing. *J Craniofac Surg* 20: 752–756. <http://dx.doi.org/10.1097/SCS.0b013e3181a2e44a>, 2009
- Wang JY, Dorafshar AH, Liu A, Groves ML, Ahn ES: The metopic index: an anthropometric index for the quantitative assessment of trigonocephaly from metopic synostosis. *J Neurosurg Pediatr*: 1–6. <http://dx.doi.org/10.3171/2016.2.PEDS15524>, 2016
- Wes AM, Paliga JT, Goldstein JA, Whitaker LA, Bartlett SP, Taylor JA: An evaluation of complications, revisions, and long-term aesthetic outcomes in nonsyndromic metopic craniosynostosis. *Plast Reconstr Surg* 133: 1453–1464. <http://dx.doi.org/10.1097/PRS.0000000000000223>, 2014
- Wilbrand J-F, Szczukowski A, Blecher J-C, Pons-Kuehnemann J, Christophis P, Howaldt H-P, et al: Objectification of cranial vault correction for craniosynostosis by three-dimensional photography. *J Craniomaxillofac Surg* 40: 726–730. <http://dx.doi.org/10.1016/j.jcms.2012.01.007>, 2012
- Wong JY, Oh AK, Ohta E, Hunt AT, Rogers GF, Mulliken JB, et al: Validity and reliability of craniofacial anthropometric measurement of 3D digital photogrammetric images. *Cleft Palate Craniofac J* 45: 232–239. <http://dx.doi.org/10.1597/06-175>, 2008